# Spectra of the Jaynes-Cummings model in presence of a second harmonic generation

**H.A.Batarfi[†], Isa A.Al-Khayat[‡], M.Sebawe Abdalla[*], and S.S.Hassan[‡].**

[†]Mathematics Department, College of Science, King AbdulAziz University, Jeddah, Saudi Arabia

[‡]Mathematics Department, College of Science, Bahrain University, P.O.Box 32038, Kingdom of Bahrain

[*]Mathematics Department, College of Science, King Saud University, P.O. Box 2455, Riyadh 11451, Saudi Arabia

**Abstract**:

Dipole and cavity field transient spectra are investigated for a modified Jaynes-Cummings (JC) model due to the presence of a second harmonic generation (SHG) cavity field. For initially de-excited atom and field in a coherent state detuning effects due to SHG affects the symmetry and splitting structure of both spectra.

## 1 Introduction

Jaynes-Cummings (JC) model [1] is a simple fundamental model in the field of quantum optics that describes the interaction of a single 2-level atom with a single mode of quantized cavity radiation field in the absence of any dissipation process by the atom or the field. The importance of this model is due to its mathematical solvability as well as to its richness with many different interesting phenomena, for example, squeezing [2], collapse-revival phenomenon [3], chaos [4], antibunching [5], and trapping states[6-9]. Advanced experimental (as well theoretical) research in the topics of micromasers and high cavity quantum electrodynamics (QED) (e.g.[10-12] ) has been inspired, in the first place, by the JC model of atom-field interaction. Extension of the JC model has been carried out to include effects like: multi-atom system, multi-level atom, multi-mode cavity field, time-dependent coupling constant, dissipation processes by the atom / the field, (e.g [13]; and references therein). Recently, we have investigated a modified Jaynes-Cummings Hamiltonian model that describes the interaction between a 2-level atom and a single

mode field in the presence of a second harmonic generation term (namely, degenerate parametric amplification) [14]. The main investigation was to study the effect of the second harmonic generation on the behavior of the atomic inversion and the entropic uncertainty. Two further quantum aspects of the model in [14], namely, field entropy as well as phase entropy have been investigated in [15]. The Hamiltonian for the modified JC model adopted in [14,15] is of the form,

$$\frac{\hat{H}}{\hbar} = \omega_f \hat{a}^\dagger \hat{a} + \frac{\omega_0}{2}\hat{\sigma}_z + \lambda(\hat{a}^\dagger + \hat{a})(\hat{\sigma}_- + \hat{\sigma}_+) + \xi(t)\hat{a}^{\dagger 2} + \xi^*(t)\hat{a}^2. \tag{1.1}$$

Here $\omega_f$ and $\omega_0$ are the field and the atomic transition frequencies respectively, and $\lambda$ is the coupling constant between the field and the atom. The operators $\hat{a}^\dagger$ and $\hat{a}$ are the creation and annihilation operators for the cavity mode such that $[\hat{a}, \hat{a}^\dagger] = 1$. The operators $\hat{\sigma}_+(\hat{\sigma}_-)$, and $\hat{\sigma}_z$ are the usual raising (lowering) and inversion operators for the two-level atomic system, satisfying $[\hat{\sigma}_z, \hat{\sigma}_\pm] = \pm 2\hat{\sigma}_\pm$ and $[\hat{\sigma}_+, \hat{\sigma}_-] = \hat{\sigma}_z$. The time-dependent complex function $\xi(t)$ is a response of the second harmonic generation (degenerate parametric amplifier) and is given by

$$\xi(t) = \frac{ik}{2}\exp(-2i\varepsilon t) \tag{1.2}$$

where $k$ is a real constant, and $\varepsilon$ is the frequency of the split photon. We may point out that the existence of the second harmonic generation term in the Hamiltonian (1) reflects possible fluctuations in the strength of the cavity field that may arise in some situations, such as: (i) fluctuations due to external signals and (ii) noise processes in the cavity due to internal reactive effects or collision with cavity walls. A simple example of a change in the cavity field is due to damping process. In this case, for a realization of this model the interaction time $t_{int}$ satisfies $t_{int} << \kappa^{-1}$, where $\kappa$ is the rate of leakage of the field out of the cavity. High $Q$-cavity with factor $Q = \omega/\kappa$ fulfills this condition. Further, the interaction time $t_{int}$ should be much shorter than the time scale of atomic spontaneous decay $\gamma^{-1}$, and long enough to allow for appreciable exchange of energy between the atom and the field and between the reservoir field modes. i.e $\lambda^{-1} << t_{int} << \gamma^{-1}, \kappa^{-1}$ (e.g.[16]). Also, the model (1) is comparable with a Hamiltonian model

describing a long-lived superposition states in cavity QED that depends on parametric amplification and engineered squeezed vacuum reservoir [17].

The aim of the present paper is to investigate both the fluorescent and transmitted spectra according to the model Hamiltonian (1). In section **II** we present an alternative analytical solution ( to that of [14]) for the system in terms of the evolution operator for two different cases: the first case when the field frequency $\omega_f$ is not equal to the splitting photon frequency $\varepsilon$ ($\omega_f \neq \varepsilon$), while in the second case $\omega_f = \varepsilon$. Analytical expressions together with the computational results for the transient dipole and cavity spectra are presented in section **III, IV** respectively. Finally a summary is given in section **V**.

## 2 The evolution operator and wave function solution

The dynamical evolution of the system described by the Hamiltonian (1) can be studied through the time evolution operator $\hat{U}(t) = exp[-i\hbar^{-1}\int_0^t \hat{H}(\grave{t})d\grave{t}]$. We briefly outline this derivation [15]. There are two cases to consider.

Case (1) ($\omega_f \neq \varepsilon$):

By introducing the time-dependent operators

$$\hat{A} = \hat{a}\exp(i\varepsilon t), \qquad \text{and} \qquad \hat{A}^\dagger = \hat{a}^\dagger \exp(-i\varepsilon t) \tag{2.1}$$

and the canonical transformation

$$\hat{A}^\dagger = \hat{B}^\dagger \cosh\phi + i\hat{B}\sinh\phi, \qquad \hat{A} = \hat{B}\cosh\phi - i\hat{B}^\dagger\sinh\phi \tag{2.2}$$

where $\hat{B}$ and $\hat{B}^\dagger$ satisfy the commutator $[\hat{B}, \hat{B}^\dagger] = 1$, the Hamiltonian (1) becomes

$$\begin{aligned}\frac{\hat{H}}{\hbar} &= \Omega\hat{B}^\dagger\hat{B} + \frac{\omega_0}{2}\hat{\sigma}_z + \lambda[(\hat{B}\cosh\phi - i\hat{B}^\dagger\sinh\phi)\exp(-i\varepsilon t) \\ &\quad +(\hat{B}^\dagger\cosh\phi + i\hat{B}\sinh\phi)\exp(i\varepsilon t)](\hat{\sigma}_- + \hat{\sigma}_+)\end{aligned} \tag{2.3}$$

where

$$\phi = \frac{1}{2}\tanh^{-1}(k/\delta), \qquad \Omega = \sqrt{\delta^2 - k^2}, \qquad \delta = (\omega_f - \varepsilon) \neq 0. \tag{2.4}$$

In the interaction picture and within the rotating wave approximation (RWA),where we neglect the energy nonconserving terms $\hat{B}\hat{\sigma}_-$ , $\hat{B}^\dagger\hat{\sigma}_+$ and terms in $\exp[\pm i(\omega_0 + \varepsilon)t]$ the Hamiltonian (5) becomes

$$\frac{V^I(t)}{\hbar} = \widetilde{g}\{\hat{B}\hat{\sigma}_+ e^{i(\Delta-\Omega)t} + \hat{B}^\dagger\hat{\sigma}_- e^{-i(\Delta-\Omega)t}\} \tag{2.5}$$

where $\widetilde{g} = \lambda\cosh\phi$,and $\Delta = \omega_0 - \varepsilon$.

The continuous map $\mathcal{E}_t^*$ describing the time evolution between the atom and the field is defined by the unitary operator generated by $\hat{H}$ such that

$$\begin{aligned} \mathcal{E}_t^* &: S_A \longrightarrow S_A \otimes S_F, \\ \mathcal{E}_t^*\rho &= \hat{U}_t\left(\rho_A(0)\otimes\rho_F(0)\right)\hat{U}_t^*, \\ \hat{U}(t) &\equiv \exp\left(-\frac{i}{\hbar}\int_0^t \hat{H}(\dot{t})d\dot{t}\right). \end{aligned} \tag{2.6}$$

We find that the evolution operator $\hat{U}(t)$ takes the following from

$$\hat{U}(t) = \begin{bmatrix} \widehat{U}_{ee} & \widehat{U}_{eg} \\ \widehat{U}_{ge} & \widehat{U}_{gg} \end{bmatrix} \tag{2.7}$$

where the matrix elements $\widehat{U}_{ij}$ in the atomic subsystem basis ( $|e\rangle$ and $|g\rangle$; the excited and the ground state respectively) are given by

$$\begin{aligned} \widehat{U}_{ee} &= \exp\left[-\frac{i(\Delta-\Omega)t}{2}\right]\left(\cos g_n t + i\frac{(\Delta-\Omega)}{2g_n}\sin g_n t\right), \\ \widehat{U}_{eg} &= -i\widetilde{g}\exp\left[-\frac{i(\Delta-\Omega)t}{2}\right]\left(\sqrt{n+1}\frac{\sin g_n t}{g_n}\right) = (\widehat{U}_{ge})^\dagger, \\ \widehat{U}_{gg} &= \exp\left[-\frac{i(\Delta-\Omega)t}{2}\right]\left(\cos g_{n-1} t + i\frac{(\Delta-\Omega)}{2g_{n-1}}\sin g_{n-1} t\right) \end{aligned} \tag{2.8}$$

where the factor $g_n$ is a Rabi frequency given by

$$g_n = \sqrt{|\widetilde{g}^2(\hat{n}+1) + \frac{1}{4}(\Delta - \Omega)^2} \tag{2.9}$$

with $\hat{n}$ is the photon number operator. Notice that the presence of the SHG affects the Rabi frequency in two aspects: Scaling the Rabi vacuum frequency by the factor $\cosh\phi$ (through $\widetilde{g}$ ) and changing $\Delta \longrightarrow \Delta - \Omega$, with $\Omega, \phi$ given in (6). The corresponding state vector $|\psi(t)\rangle$ for the system is expanded as follows,

$$|\psi(t)\rangle = \sum_{n=0}^{\infty}\{C_{e,n}(t)|e,n\rangle + C_{g,n+1}(t)|g,n+1\rangle\} \tag{2.10}$$

and is readily obtained via $|\psi(t)\rangle = \hat{U}(t)|\psi(0)\rangle$, with $\hat{U}(t)$ given by (9). Thus the probability amplitudes are given by

$$\begin{aligned} C_{e,n}(t) &= \exp[-\frac{i}{2}(\Delta - \Omega)t]\left[\left(C_{e,n}(0)(\cos g_n t + i\frac{(\Delta - \Omega)}{2g_n}\sin g_n t)\right)\right. \\ &\left. -i\left(\frac{\widetilde{g}\sqrt{n+1}}{g_n}\sin g_n t C_{g,n+1}(o)\right)\right], \end{aligned}$$

and

$$\begin{aligned} C_{g,n+1}(t) &= \exp[\frac{i}{2}(\Delta - \Omega)t]\left[\left(C_{g,n+1}(0)(\cos g_n t - i\frac{(\Delta - \Omega)}{2g_n}\sin g_n t)\right)\right. \\ &\left. -i\left(\frac{\widetilde{g}\sqrt{n+1}}{g_n}\sin g_n t C_{e,n}(o)\right)\right]. \end{aligned} \tag{2.11}$$

**Case II** ($\omega_f = \varepsilon$):

Note that the present case is *not* the limiting case of $\delta \longrightarrow 0$ as seen from equation (6). So, we set $\varepsilon = \omega_f$ in equation (2) and follow the same procedure as in case (I) and define the time-dependent operators $\hat{A}_1$ and $\hat{A}_1^\dagger$,

$$\hat{A}_1 = \hat{a}\exp(i\omega_f t), \qquad \text{and} \qquad \hat{A}_1^\dagger = \hat{a}^\dagger\exp(-i\omega_f t). \tag{2.12}$$

The Hamiltonian (1) in the interaction picture within the RWA frame then takes the form

$$\frac{V^I(t)}{\hbar} = \lambda\cosh kt\left(\hat{A}_1\hat{\sigma}_+\exp(-i\Delta t) + \hat{A}_1^\dagger\hat{\sigma}_-\exp(i\Delta t)\right). \tag{2.13}$$

Now using equations (8) and (9) together with equation (15), we get for $\Delta = 0$, the matrix elements of the evolution operator in (9) as,

$$\begin{aligned}
\widehat{U}_{ee} &= I_0(\bar{g}_n) + 2\sum_{r=1}^{\infty}(-)^r I_{2r}(\bar{g}_n)\cosh(2rkt), \\
\widehat{U}_{eg} &= -2i\left(\sum_{r=0}^{\infty}(-)^r I_{(2r+1)}(\bar{g}_n)\sinh[(2r+1)kt]\right), \qquad (2.14) \\
\widehat{U}_{gg} &= \left(I_0(\bar{g}_n) + 2\sum_{r=1}^{\infty}(-)^r I_{2r}(\bar{g}_n)\cosh(2rkt)\right)
\end{aligned}$$

where $\bar{g}_n = (\lambda/k)\times\sqrt{\hat{n}+1}$ is a modified Rabi frequency and $I_n(.)$ is the modified Bessel function of order $n$. The corresponding probability amplitudes in (12) then has the form,

$$\begin{aligned}
C_{e,n}(t) &= \left(I_0(\overline{g}) + 2\sum_{r=1}^{\infty}(-)^r I_{2r}(\overline{g})\cosh(2rkt)\right) C_{e,n}(0) \\
&\quad -2i\left(\sum_{r=0}^{\infty}(-)^r I_{(2r+1)}(\overline{g})\sinh[(2r+1)kt]\right) C_{g,n+1}(0)
\end{aligned}$$

and

$$\begin{aligned}
C_{g,n+1}(t) &= \left(I_0(\overline{g}) + 2\sum_{r=1}^{\infty}(-)^r I_{2r}(\overline{g})\cosh(2rkt)\right) C_{g,n+1}(0) \\
&\quad -2i\left(\sum_{r=0}^{\infty}(-)^r I_{(2r+1)}(\overline{g})\sinh[(2r+1)kt]\right) C_{e,n}(0). \qquad (2.15)
\end{aligned}$$

In the following two sections we utilize the solutions (13),(17) to calculate and investigate both the dipole (i.e. fluorescent) and cavity (i.e transmitted) transient spectra.

# 3 The dipole Spectrum

The transient spectrum is given by [18]

$$S(t,D,\Gamma) = 2\Gamma \int_{-\infty}^{t} dt_1 \int_{-\infty}^{t} dt_2 e^{(-\Gamma+iD)(t-t_1)} e^{(-\Gamma-iD)(t-t_2)} \langle \hat{C}_+(t_1)\hat{C}_-(t_2)\rangle \tag{3.1}$$

where $\Gamma$ is the Fabry-Perot detector width. The operators $\hat{C}_{\pm}(t)$ represent the atomic operators $\hat{\sigma}_{\pm}$ for the case of dipole spectrum, while they represent the field creation and annihilation operators $\hat{a}^{\dagger}$ and $\hat{a}$ for the case of cavity (i.e.transmitted ) spectrum. The parameter $D = (\omega - \omega_0)$ is the detector's detuning parameter from the atomic frequency in the case of dipole spectrum. In the case of cavity spectrum $D = (\omega - \omega_f)$.

We consider the combined initial state of the (atom $\oplus$ field) system to be $|g,\alpha\rangle$ where $|\alpha\rangle = \exp(-\frac{1}{2}|\alpha|^2)\sum_{n=0}^{\infty}\frac{\alpha^n}{\sqrt{n!}}|n\rangle$ is the coherent field state. The dipole-dipole correlation function $\langle \hat{C}_+(t_1)\hat{C}_-(t_2)\rangle = \langle \hat{\sigma}_+(t_1)\hat{\sigma}_-(t_2)\rangle$ appearing in (18) is then given by

$$\langle \hat{\sigma}_+(t_1)\hat{\sigma}_-(t_2)\rangle = \exp(-|\alpha|^2)\sum_{\acute{n},\acute{m}=0}^{\infty}\frac{(\alpha)^{\acute{n}}(\alpha^*)^{\acute{m}}}{\sqrt{\acute{n}!\acute{m}!}}\langle g,\acute{n}|\hat{\sigma}_+(t_1)\hat{I}\hat{\sigma}_-(t_2)|g,\acute{m}\rangle, \tag{3.2}$$

where we have inserted the completeness relation

$$\hat{I} = \sum_{n=0}^{\infty}[|e,n\rangle\langle e,n| + |g,n+1\rangle\langle g,n+1|]. \tag{3.3}$$

For initial atomic ground state$|g\rangle$, equation (19) has the form

$$\langle \hat{\sigma}_+(t_1)\hat{\sigma}_-(t_2)\rangle = \exp(-|\alpha|^2)\sum_{n=0}^{\infty}\left(I_{n,1}(t_1)\acute{I}_{n,1}(t_2) + I_{n,2}(t_1)\acute{I}_{n,2}(t_2)\right) \tag{3.4}$$

where:

$$
\begin{aligned}
I_{n,1}(t_1) &= \sum_{\dot{n}=0}^{\infty} \frac{\alpha^{\dot{n}}}{\sqrt{\dot{n}!}} \langle g, \dot{n}|\hat{\sigma}_+(t_1)|e, n\rangle, \\
\acute{I}_{n,1}(t_2) &= \sum_{\ddot{n}=0}^{\infty} \frac{(\alpha^*)^{\ddot{n}}}{\sqrt{\ddot{n}!}} \langle e, \ddot{n}|\hat{\sigma}_-(t_2)|g, \ddot{n}\rangle, \\
I_{n,2}(t_1) &= \sum_{\dot{n}=0}^{\infty} \frac{\alpha^{\dot{n}}}{\sqrt{\dot{n}!}} \langle g, \dot{n}|\hat{\sigma}_+(t_1)|g, n+1\rangle, \\
\acute{I}_{n,2}(t_2) &= \sum_{\dot{n}=0}^{\infty} \frac{(\alpha^*)^{\ddot{n}}}{\sqrt{\ddot{n}!}} \langle g, n+1|\hat{\sigma}_-(t_2)|g, \ddot{n}\rangle
\end{aligned} \tag{3.5}
$$

Now, any of the four quantities in equation (22) can be calculated as follows. For example,

$$
\begin{aligned}
I_{n,1}(t_1) &= \sum_{\dot{n}=0}^{\infty} \frac{\alpha^{\dot{n}}}{\sqrt{\dot{n}!}} \langle g, \dot{n}|e^{-iHt_1}\hat{\sigma}_+(0)e^{iHt_1}|e, n\rangle, \\
&= \sum_{\dot{n}=0}^{\infty} \frac{\alpha^{\dot{n}}}{\sqrt{\dot{n}!}} \langle \psi(t_1)|_{g,\dot{n}}|\hat{\sigma}_+(0)|\psi(t_1)\rangle_{e,n}
\end{aligned} \tag{3.6}
$$

where $|\psi(t_1)\rangle_{e,n}$ is the state vector at $(t_1)$ given the specific initial state $|e, n\rangle$ and it is given from equation (12) by

$$
|\psi(t_1)\rangle_{e,n} = \{C_{e,n}(t_1)|_e|e, n\rangle + C_{g,n+1}(t_1)|_e|g, n+1\rangle\},
$$

and similarly,

$$
\langle\psi(t_1)|_{g,\dot{n}} = C^*_{e,\dot{n}}(t_1)|_g\langle e, \dot{n}| + C^*_{e,\dot{n}+1}(t_1)|_g\langle g, \dot{n}+1|
$$

so,

$$
\langle\psi(t_1)|_{g,\dot{n}}|\hat{\sigma}_+(0)|\psi(t_1)\rangle_{e,n} = C_{g,n+1}(t_1)|_e C^*_{e,\dot{n}}(t_1)|_g \delta_{\dot{n},n+1}.
$$

Hence,

$$
I_{n,1}(t_1) = \frac{\alpha^{n+1}}{\sqrt{(n+1)!}} C_{g,n+1}(t_1)|_c C^*_{e,\dot{n}}(t_1)|_g.
$$

In a similar manner we have

$$\begin{aligned} I_{n,2}(t_1) &= \frac{(\alpha^*)^{n+1}}{\sqrt{(n+1)!}} C_{g,n+1}(t_1)|_g C^*_{e,n+1}(t_1)|_g \\ \dot{I}_{n,1}(t_2) &= I^*_{n,1}(t_2), \qquad \dot{I}_{n,2}(t_2) = I^*_{n,2}(t_2) \end{aligned} \tag{3.7}$$

where, eg, $C_{g,n+1}(t_1)|_e$ is obtained from the corresponding expression $C_{g,n+1}(t_1)$ (equation (13) or (17)- depends on $\omega_f \neq \varepsilon$ or $\omega_f = \varepsilon$ ) by putting the initial conditions $C_{g,n+1}(0) = 0$, $C_{e,n}(0) = 1$. Thus, equation (21) takes the form

$$\langle \hat{\sigma}_+(t_1)\hat{\sigma}_-(t_2)\rangle = \exp(-|\alpha|^2) \sum_{n=0}^{\infty} \frac{|\alpha|^{2(n+1)}}{(n+1)!} \left(a_n(t_1)a^*_n(t_2) + b_n(t_1)b^*_n(t_2)\right) \tag{3.8}$$

with

$$a_n(t) = C_{g,n+1}(t)|_e C^*_{e,n+1}(t)|_g, \qquad b_n(t) = C_{g,n+1}(t)|_g C^*_{e,n+1}(t)|_g. \tag{3.9}$$

The expression (25) for the dipole auto-correlation function reduces to that obtained by Narozhny et al [3] for the JC model. Inserting equation (25) into equation (18) we get the dipole spectrum $S_d$ in the form,

$$S_d(t, D, \Gamma) = 2\Gamma \exp(-\bar{n}) \sum_{n=0}^{\infty} \frac{(\bar{n})^{(n+1)}}{(n+1)!} \left[|\mathcal{A}_n(t)|^2 + |\mathcal{B}_n(t)|^2\right], \tag{3.10}$$

where $\bar{n} = |\alpha|^2$ and

$$\begin{aligned} \mathcal{A}_n(t) &= \int_{-\infty}^{t} a_n(\dot{t}) \exp[(-\Gamma + iD)(t - \dot{t})] d\dot{t}, \\ \mathcal{B}_n(t) &= \int_{-\infty}^{t} b_n(\dot{t}) \exp[(-\Gamma + iD)(t - \dot{t})] d\dot{t}. \end{aligned} \tag{3.11}$$

The explicit analytical expression for the functions $\mathcal{A}_n(t)$ and $\mathcal{B}_n(t)$ in the two cases of $\omega_f \neq \varepsilon$, and $\omega_f = \varepsilon$ are given in the appendix, together with the corresponding expression for the JC model. The computational results for the dipole spectrum in equation (27) are presented in figs.(1-3) where we note the following:-

**(i) JC model:** For time $t = 15\lambda^{-1}$ and detector's width $\Gamma = \lambda$ (at exact atomic resonance $\Delta = 0$ ) symmetric 3-peak structure develops with increasing field input $\bar{n}$ ; fig.1: central peak at $D = 0$, and two-side peaks at $D/\lambda \simeq 2\lambda(\bar{n}+2)^{\frac{1}{2}}$. Also, for fixed $\bar{n}$ this symmetric 3-peak profile survives with increasing $t$.

**(ii) Modified JC model with** $(\omega_f \neq \varepsilon)$: For splitting frequency mismatch $\delta = 0.5\lambda, \Gamma = \lambda, \Delta = 0$ and for second harmonic generation coupling parameter $k = 0.3\lambda$ at $t = 0$, fig.(2a), the spectrum starts for small $\bar{n} = 0.1$ as a single Lorentzian peak and develops to symmetric three-peak spectrum as $\bar{n}$ gets larger $(= 15)$. For $t = 10\lambda^{-1}$, fig.(2b), the dominant central peak for small $\bar{n}$ develops to 3-peak spectrum as $\bar{n}$ increases with weight of central peak much reduced. For atomic detuning $\Delta = 5\lambda$.the same symmetric structure occurs but the whole spectrum shifts to the right by the value of $\Delta$.

**(iii) Modified JC model with** $(\omega_f = \varepsilon)$: At $t = 0$, $k = 0.1\lambda$, $\Gamma = 0.5\lambda$, $\bar{n} = 20$ the spectrum is a single central peak with narrowed spike (fig.(3a)) ,but for larger $k = 0.8\lambda$ this central peak broadens (fig.(3b)). For larger $\Gamma = 3\lambda$ two-side peaks emerge (fig.(3c)). For time $t > \lambda^{-1}$ the central peak further broadens with the merge of the side peaks.

# 4 The Cavity spectrum

Following similar procedure to the calculation of the dipole auto-correlation function in equation (25), we get the auto-correlation function for the field operators in the form (assuming the initial combined state is $|g,\alpha\rangle$),

$$\begin{aligned}\langle \hat{a}^\dagger(t_1)\hat{a}(t_2)\rangle &= e^{-|\alpha|^2}\sum_{\acute{n},\ddot{n}=0}^{\infty}\frac{(\alpha)^{\acute{n}}(\alpha^*)^{\ddot{n}}}{\sqrt{\acute{n}!\ddot{n}!}}\langle g,\acute{n}|\hat{a}^\dagger(t_1)\hat{a}(t_2)|g,\ddot{n}\rangle \\ &= e^{-\bar{n}}\sum_{n=0}^{\infty}\frac{(\bar{n})^{n+1}}{(n+1)!}\left[c_n(t_1)c_n^*(t_2)+d_n(t_1)d_n^*(t_2)\right] \qquad (4.1)\end{aligned}$$

where

$$\begin{aligned}c_n(t) &= \left[\sqrt{n+1}C^*_{e,n+1}(t)|_g C_{e,n}(t)|_e + \sqrt{n+2}C^*_{g,n+2}(t)|_g C_{g,n+1}(t)|_e\right], \\ d_n(t) &= \left[\sqrt{n+1}C^*_{e,n+1}(t)|_g C_{e,n}(t)|_g + \sqrt{n+2}C^*_{g,n+2}(t)|_g C_{g,n+1}(t)|_g\right] \qquad (4.2)\end{aligned}$$

Hence the cavity spectrum $S_c(t, D, \Gamma)$ has the form

$$S_c(t, D, \Gamma) = 2\Gamma e^{-\bar{n}} \sum_{n=0}^{\infty} \frac{(\bar{n})^{n+1}}{(n+1)!} \left( |\mathcal{C}_n(t)|^2 + |\mathcal{D}_n(t)|^2 \right), \tag{4.3}$$

where

$$\begin{aligned} \mathcal{C}_n(t) &= \int_{-\infty}^{t} c_n(\acute{t}) \exp[(-\Gamma + iD)(t - \acute{t})] d\acute{t}, \\ \mathcal{D}_n(t) &= \int_{-\infty}^{t} d_n(\acute{t}) \exp[(-\Gamma + iD)(t - \acute{t})] d\acute{t}. \end{aligned} \tag{4.4}$$

The explicit analytical expressions for the functions $\mathcal{C}_n(t)$ and $\mathcal{D}_n(t)$ in the two cases of $\omega_f \neq \varepsilon$, and $\omega_f = \varepsilon$, together with the corresponding expression for the ordinary JC model, are given in the appendix.

The computational results for the cavity spectrum in equation (31) are presented in figs.(4-6) where we note the following:

(i) **JC model**: For $t = 10\lambda^{-1}$ a single central peak develops with increasing $\bar{n}$ (fig.4).

(ii) **Modified JC model with** $(\omega_f \neq \varepsilon)$: For $t = 0$ and $10\lambda^{-1}$, $\Gamma = \lambda$, $k = 0.3\lambda$, $\Delta = 0$, $\delta = 0.5\lambda$ and as $\bar{n}$ increases the spectrum is asymmetric and has a central peak (of weight increased with $\bar{n}$ ) and one side band of lesser weight, (fig.5a,b). The asymmetry here is due to the superposition of Lorentzians of different weights (the coefficients $g_{n,\pm}$ ) and different location (terms in $\gamma_n^{\pm}, \eta_n^{\pm}$) in the expressions for $\mathcal{C}_n(t)$, and $\mathcal{D}_n(t)$ in equations in the appendix (A.3), (A.4).

(iii) **Modified JC model with** $(\omega_f = \varepsilon)$: For $k = 0.1\lambda$, $\Gamma = 0.5\lambda$, $\bar{n} = 20$ and at $t = 0$, the spectrum is a single broad Lorentzian with spike at $D = 0$ -fig.(6a)- that vanishes as $t$ increases ( $t = 5\lambda^{-1}$ ), fig.(6b). For larger $k = 0.8\lambda$ and $\Gamma = 3\lambda$ two side peaks emerge at $t = 0$ -fig.(6c)- but for increasing $t = \lambda^{-1}$ the central peak is broadened with the two side peaks move towards the center fig.(6d).

# 5 Summary

The transient dipole and cavity spectra of a modified JC model have been calculated and examined in detail. The modified JC model [14,15] considered

here is the usual JC model in a high-$Q$ cavity but with the presence of a second harmonic generation field of the single cavity mode which is *not* coupled to the atom ( coupling of this " background" second harmonic field is ignored within rotating wave approximation [14]). Based on the derived analytical solutions and for initially ground state atom and field in a coherent state ( of average photon number $\bar{n}$ ) our main computational investigation for both spectra are :-

(a) **Dipole spectrum**

In the case when the splitting photon frequency $\varepsilon$ is not equal to the cavity field frequency $\omega_f$ ($\omega_f \neq \varepsilon$) the effect of the second harmonic field shows that the spectrum develops from a single Lorentzian peak to the usual symmetric 3-peak Mollow structure as $\bar{n}$ increases. Further increase of $\bar{n}$ for time $t \gg \lambda^{-1}$ ($\lambda$ = coupling constant of atom and first harmonic cavity field) reduces the weight of the central resonant peak significantly. For the case where $\omega_f = \varepsilon$, the initial spectrum is essentially a single spiked resonant peak which broadens with increasing value of the (second harmonic field) parameter $k$- but for increasing $t > \lambda^{-1}$ the tendency of appearance of two side-peak structure vanishes and the central peak further broadens.

(b) **Cavity spectrum**

In the case of $\omega_f \neq \varepsilon$ and for large $\bar{n}$, and $t \geq 0$ the spectrum is asymmetric (one central resonant peak at $D = 0$ and one side peak at $D \simeq \lambda\bar{n}$ ). This asymmetry is due to the superposition of Lorentzians of same width but of different heights and locations. The presence of the off-resonant second harmonic field induces these $k$-dependent detuning-like parameters $\gamma_n^{(\pm)}, \eta_n^{(\pm)}$ in the number (cavity field) spectrum. For the case of $\omega_f = \varepsilon$ the spectrum is symmetric and develops from a broad Lorentzian with spike structure and for increasing value of $k$ two side-peak structure near the centre appears with increasing weight for larger time $t \gg \lambda^{-1}$.

## Appendix (A).

i) Here we give the explicit expressions for the functions $\mathcal{A}_n$,$\mathcal{B}_n$,$\mathcal{C}_n$, and $\mathcal{D}_n$ given in equations (28) and (32), in the two cases of $\omega_f \neq \varepsilon$ and $\omega_f = \varepsilon$.

**Case of** $(\omega_f \neq \varepsilon)$:

$$\mathcal{A}_n(t) = \frac{\cosh^2\phi\sqrt{(n+1)(n+2)}}{4g_ng_{n+1}}\left[\left(\frac{\exp(-i\xi_n^{(-)}t)}{\Gamma - i\xi_n^{(-)}} + \frac{\exp(-i\xi_n^{(+)}t)}{\Gamma - i\xi_n^{(+)}}\right) - \left(\frac{\exp(-i\zeta_n^{(-)}t)}{\Gamma - i\zeta_n^{(-)}} + \frac{\exp(-i\zeta_n^{(+)}t)}{\Gamma - i\zeta_n^{(+)}}\right)\right], \tag{A1}$$

$$\mathcal{B}_n(t) = \beta_n\frac{\cosh\phi\sqrt{(n+2)}}{8g_ng_{n+1}}\left[\left(\frac{\exp(-i\zeta_n^{(-)}t)}{\Gamma - i\zeta_n^{(-)}} + \frac{\exp(-i\zeta_n^{(+)}t)}{\Gamma - i\zeta_n^{(+)}}\right) - \left(\frac{\exp(-i\xi_n^{(-)}t)}{\Gamma - i\xi_n^{(-)}} + \frac{\exp(-i\xi_n^{(+)}t)}{\Gamma - i\xi_n^{(+)}}\right)\right] \tag{A2}$$

$$\mathcal{C}_n(t) = \frac{\cosh\phi\sqrt{(n+1)(n+2)}}{4g_ng_{n+1}}\left[g_{n,+}\left(\frac{\exp(-i\gamma_n^{(+)}t)}{\Gamma - i\gamma_n^{(+)}} - \frac{\exp(-i\gamma_n^{(-)}t)}{\Gamma - i\gamma_n^{(-)}}\right) + g_{n,-}\left(\frac{\exp(-i\eta_n^{(+)}t)}{\Gamma - i\eta_n^{(+)}} - \frac{\exp(-i\eta_n^{(-)}t)}{\Gamma - i\eta_n^{(-)}}\right)\right], \tag{A3}$$

and

$$\mathcal{D}_n(t) = \frac{\sqrt{(n+2)}}{4g_{n+1}}\left[g_{n,+}\left(\frac{\exp(-i\gamma_n^{(-)}t)}{\Gamma - i\gamma_n^{(-)}} + \frac{\exp(-i\eta_n^{(+)}t)}{\Gamma - i\eta_n^{(+)}}\right) + g_{n,-}\left(\frac{\exp(-i\gamma_n^{(+)}t)}{\Gamma - i\gamma_n^{(+)}} - \frac{\exp(-i\eta_n^{(-)}t)}{\Gamma - i\eta_n^{(-)}}\right)\right] + \frac{\sqrt{(n+2)}}{8g_{n+1}}(\Delta - \Omega)\left[\frac{\exp(-i\gamma_n^{(+)}t)}{\Gamma - i\gamma_n^{(+)}} - \frac{\exp(-i\gamma_n^{(-)}t)}{\Gamma - i\gamma_n^{(-)}}\right] \tag{A4}$$

where

$$\begin{aligned} \xi_n^{(\pm)} &= (D - \Delta + \Omega \pm g_{n,-}), \qquad \zeta_n^{(\pm)} = (D - \Delta + \Omega \pm g_{n,+}), \\ \beta_n &= (2g_n - \Delta + \Omega), \qquad g_{n,\pm} = (g_n \pm g_{n+1}), \\ \gamma_n^{(\pm)} &= (D \pm g_{n,-}), \qquad \eta_n^{(\pm)} = (D \pm g_{n,+}). \end{aligned} \tag{A5}$$

**Case of** $(\omega_f = \varepsilon)$:

$$\mathcal{A}_n(t) = \frac{1}{2}\left[\frac{I_0(\bar{g}_{n,-}) - I_0(\bar{g}_{n,+})}{\Gamma - iD} + \sum_{r=1}^{\infty}(-)^r\{I_{2r}(\bar{g}_{n,-}) - I_{2r}(\bar{g}_{n,+})\} \times \left(\frac{\exp(2rkt)}{\Gamma + 2rk - iD} + \frac{\exp(-2rkt)}{\Gamma - 2rk - iD}\right)\right] \quad \text{(A6)}$$

and

$$\mathcal{B}_n(t) = \frac{1}{2}\sum_{r=1}^{\infty}(-)^r\{I_{2r+1}(\bar{g}_{n,+}) - I_{2r+1}(\bar{g}_{n,-})\} \times \left[\frac{\exp[(2r+1)kt]}{\Gamma + (2r+1)k - iD} + \frac{\exp[-(2r+1)kt]}{\Gamma - (2r+1)k - iD}\right], \quad \text{(A7)}$$

$$\mathcal{C}_n(t) = \frac{i}{2}\sum_{r=0}^{\infty}(-)^r\left[\left(\sqrt{n+1} - \sqrt{n+2}\right) I_{2r+1}(\bar{g}_{n,+}) - \left(\sqrt{n+1} + \sqrt{n+2}\right) I_{2r+1}(\bar{g}_{n,-})\right] \times \left(\frac{\exp[(2r+1)kt]}{\Gamma + (2r+1)k - iD} - \frac{\exp[-(2r+1)kt]}{\Gamma - (2r+1)k - iD}\right) \quad \text{(A8)}$$

and

$$\mathcal{D}_n(t) = \frac{1}{2(\Gamma - iD)}\left[\left(\sqrt{n+1} + \sqrt{n+2}\right) I_0(\bar{g}_{n,-}) - \left(\sqrt{n+1} - \sqrt{n+2}\right) I_0(\bar{g}_{n,+})\right] + \frac{1}{2}\sum_{r=0}^{\infty}(-)^r\left[\left(\sqrt{n+1} + \sqrt{n+2}\right) I_{2r}(\bar{g}_{n,-}) - \left(\sqrt{n+1} - \sqrt{n+2}\right) I_{2r}(\bar{g}_{n,+})\right] \times \left(\frac{\exp[(2r+1)kt]}{\Gamma + 2rk - iD} + \frac{\exp[-(2r+1)kt]}{\Gamma - 2rk - iD}\right). \quad \text{(A9)}$$

where $\bar{g}_{n,\pm} = \bar{g}_n \pm \bar{g}_{n+1}$.

ii) Here we give, for completeness, the corresponding expressions for the functions $\mathcal{A}_n(t)$, $\mathcal{B}_n(t)$ (appearing in the dipole spectrum $S_d$) and the

functions $\mathcal{C}_n(t)$, $\mathcal{D}_n(t)$ (appearing in the cavity spectrum $S_c$) for the JC model. These expressions can be obtained by talking the limit $k \longrightarrow 0$ in equations (A1-A4), noting that from equation (6) that $\phi = \frac{1}{2}\tanh^{-1}(k/\delta)$, $\Omega = \sqrt{\delta^2 - k^2}$.

$$\mathcal{A}_n(t) = \frac{1}{4}\left[\left(\frac{\exp[-i(D-h_{n+1,-})t]}{\Gamma - i(D-h_{n+1,-})} - \frac{\exp[-i(D+h_{n+1,+})t]}{\Gamma - i(D+h_{n+1,+})}\right) + (h_{n+1,\mp} \longrightarrow -h_{n+1,\mp})\right], \tag{A10}$$

$$\mathcal{B}_n(t) = \frac{1}{4}\left[\left(\frac{\exp[-i(D-h_{n+1,+})t]}{\Gamma - i(D-h_{n+1,+})} + \frac{\exp[-i(D+h_{n+1,-})t]}{\Gamma - i(D+h_{n+1,-})}\right) - (h_{n+1,\mp} \longrightarrow -h_{n+1,\mp})\right], \tag{A11}$$

$$\mathcal{C}_n(t) = \frac{1}{4}\left[(\sqrt{n+1}-\sqrt{n+2})\left(\frac{\exp[-i(D-h_{n+1,-})t]}{\Gamma - i(D-h_{n+1,+})} - (h_{n+1,+} \longrightarrow -h_{n+1,+})\right) -(\sqrt{n+1}+\sqrt{n+2})\left(\frac{\exp[-i(D-h_{n+1,-})t]}{\Gamma - i(D-h_{n+1,-})} - (h_{n+1,-} \longrightarrow -h_{n+1,-})\right)\right] \tag{A12}$$

and

$$\mathcal{D}_n(t) = \frac{1}{4}\left[(\sqrt{n+1}+\sqrt{n+2})\left(\frac{\exp[-i(D-h_{n+1,-})t]}{\Gamma - i(D-h_{n+1,-})} + (h_{n+1,-} \longrightarrow -h_{n+1,-})\right) - (\sqrt{n+1}-\sqrt{n+2})\left(\frac{\exp[-i(D+h_{n+1,+})t]}{\Gamma - i(D+h_{n+1,+})} + (h_{n+1,+} \longrightarrow -h_{n+1,+})\right)\right] \tag{A13}$$

where,

$$h_{n+1,\pm} = h_{n+1} \pm h_{n+2} \quad ; \quad h_n = \sqrt{\Delta^2 + \lambda^2(n+1)}. \tag{A14}$$

Note that, it can be checked from the expressions (A.10) -(A.13) that for the JC model with atom initially in its ground state both dipole and cavity spectra are symmetric (the same is shown with atom initially in its excited state [19]).

**Acknowledgement:**
One Of us (M.S.A.) is grateful for the financial support of the project Math 2005/32 of the Research Centre, College of Science, King Saud University.

# References

[1] E.T.Jaynes and F.W.Cummings,Comparison of quantum and semiclassical radiation theories with application to the beam maser, Proc.IEEE **51**,89-109(1963).

[2] P.Meystre,and M.S.Zubairy,Squeezed states in the Jaynes-Cummings model , Phys.Lett.A**89**,390-392(1982); J. R. Kuklinski, and J.L.Madajczyk, Strong squeezing in the Jaynes-Cummings model,Phys.Rev.A **37**,3175-3178(1988).

[3] J.H.Eberly, N.B.Narozhny,and J.J.Sanchez-Mondragan,Periodic Spontaneous Collapse and Revival in a Simple Quantum Model, Phys.Rev.Lett.**44**,1323-1326(1980); N.B.Narozhny,J.J.Sanchez-Mondragan,andJ.H.Eberly,Coherence versus incoherence: Collapse and revival in a simple quantum model, Phys.Rev.A.,**23,** 236-247(1981).

[4] P.W.Milonni,J.R.Ackerhalt, and H.W.Galbraith,Chaos in the Semiclassical N-Atom Jaynes-Cummings Model: Failure of the Rotating-Wave Approximation, Phys.Rev.Lett **50**,966-969(1983).

[5] R.G.Short,and L.Mandel,Observation of Sub-Poissonian Photon Statistics, Phys.Rev.Lett.**51**,384-387(1983);F.Diedrich,and H.Walther,Nonclassical radiation of a single stored ion, Phys.Rev.Lett **58**,203-206(1987).

[6] J.J.Slosser,P.Meystre,and S.L.Braunstein,Harmonic oscillator driven by a quantum current, Phys.Rev.Lett.**63**,934-937(1989).

[7] J.J.Slosser,and P.Meystre,Tangent and cotangent states of the electromagnetic field, Phys.Rev.A **41**,3867-74(1990).

[8] J.Gea-Banacloche,Collapse and revival of the state vector in the Jaynes-Cummings model: An example of state preparation by a quantum

apparatus,Phys.Rev.Lett.**65**,3385-3388(1990);Atom- and field-state evolution in the Jaynes-Cummings model for large initial fields, Phys.Rev.A **44**,5913-5931(1991).

[9] S.J.D.Phoenix,and P.L.Knight,Establishment of an entangled atom-field state in the Jaynes-Cummings model,Phys.Rev.A **44** ,6023-6029(1991);ibid Comment on "Collapse and revival of the state vector in the Jaynes-Cummings model: An example of state preparation by a quantum apparatus" Phys.Rev.Lett **66**,2833-2837(1991);ibid, Fluctuations and entropy in models of quantum optical resonance Ann.Phys.(N.Y)**186**,381-407(1988).

[10] S.Haroche,in "New Trends in Atomic physics,proc.of the Les Houches Summer School of Theoretical Physics" **XXXVIII**,eds:G.Grynberg and R.Stora (North Holland, Amsterdam,1984),and Refs. therein; M.Brune, J.M.Raimond, P.Goy,L.Davidovich and S.Haroche, Realization of a two-photon maser oscillator,Phys.Rev.Lett.**59**,1899-1902(1987).

[11] D.Meschede,H.Walker,G.Muller,One-Atom Maser, Phys.Rev.Lett.**54**,551-554 (1985);G. Rempe, H. Walker, N. Klein,Observation of quantum collapse and revival in a one-atom maser,Phys.Rev.Lett.**58**,353-356 (1987).

[12] D. Kleppner, **u (3)**-Boson Model of Nuclear Collective Motion, Phys. Rev. Lett. **47**, 223-226 (1981); T. R. Gentile, B. J. Hnghey, and D. Kleppner, Experimental study of one- and two-photon Rabi oscillations, Phys. Rev. A **40**, 5103-5115 (1989).

[13] B.W.Shore and P.L. Knight, The Jaynes-Cummings Model,J. Mod. Opt. **40**,1195-1238 (1993); V.V. Dodonov,W. D. Jose, and S. S. Mizrahi, Dispersive limit of the dissipative Jaynes–Cummings model with a squeezed reservoir, J.Opt.B:Quantum Semiclass. Opt. **5**, **S567** (2003); S.M.Chumakov, A.B.Klimov and M. Kozierowski, 2003"Theory of Non-classical States of Light ed V.V.Dodonov and V. I. Man'ko (London:Taylor and Francis) **p** 319; V.Buzek,I.Jex and M.Brisndova, Jaynes-Cummings Model with displaced number states, Int.J.Mod.Phys.B5,797-814(1991).

[14] M.S.Abdalla,S.S.Hassan,and M.Abdel-Aty,Entropic uncertainty in the Jaynes–Cummings model in presence of a second harmonic generation, Opt.Commun.**244**,431-443(2005).

[15] M.S.Abdalla,M.Abdel-Aty,and A.-S.F.Obada, Sensitive response of the quantum entropies to Jaynes-Cummings model in presence of a second harmonic generation, Int.J.Theor.Phys.**46**, 637(2007).

[16] R.R.Puri,"Mathematical Methods of Quantum Optics"Springer Series in Optical Sciences Vol.**79**(2001),Chapters 7,8.

[17] C.J.Villas-Bôas,F-
R.de Paula, R.M.Serra, M.H.Y.Moussa, J.Opt.B:Quantum Semiclass. Opt.**5**,391(2003).

[18] K.Wodkiewicz and J.H.Eberly, Effects of hidden transient noise processes on multiphoton absorption, J.Opt.Soc.Am.**3**,629(1986).

[19] T.Nasreen and M.S.K.Razmi, Atomic emission and cavity field spectra for a two-photon Jaynes - Cummings model in the presence of Stark shift, J.Opt.Soc.Am.B **10**,1292 (1993).

Figure Captions:

(1): The dipole spectrum $S_d$, for JC model against the normalized detuning parameter; $\overline{D} = D/\lambda$ at $t = 15\lambda^{-1}, \Gamma = \lambda, \Delta = 0$ and various $\bar{n}$.

(2): (a) The 3-dimensional plot of the dipole spectrum $S_d$ against $\overline{D}, \bar{n}$ for the modified JC model with off-resonant SHG field ($\delta = 0.5\lambda$) at $t = 0, \Gamma = \lambda, \Delta = 0, k = 0.3\lambda$. (b) As (a) but for $t = 10\lambda^{-1}$.

(3) (a),(b),(c). The dipole spectrum $S_d$ (log-scale) for the modified JC model with resonant SHG field ($\delta = 0$) at $t = 0, \Delta = 0, \bar{n} = 20$ and for various values of $(k, \Gamma)$.

(4) The cavity spectrum $S_c$, for the JC model at $t = 15\lambda^{-1}, \Gamma = \lambda, \Delta = 0$ and various $\bar{n}$.

(5): (a) The cavity spectrum $S_c$, for the modified JC model and data as in fig.(2a). (b) As (a) but $t = 10\lambda^{-1}$ .

(6): (a)-(d) The cavity spectrum $S_c$ (log-scale) for the modified JC model ($\delta = 0$) for various values of $(t, k, \Gamma)$.

Fig.(1)

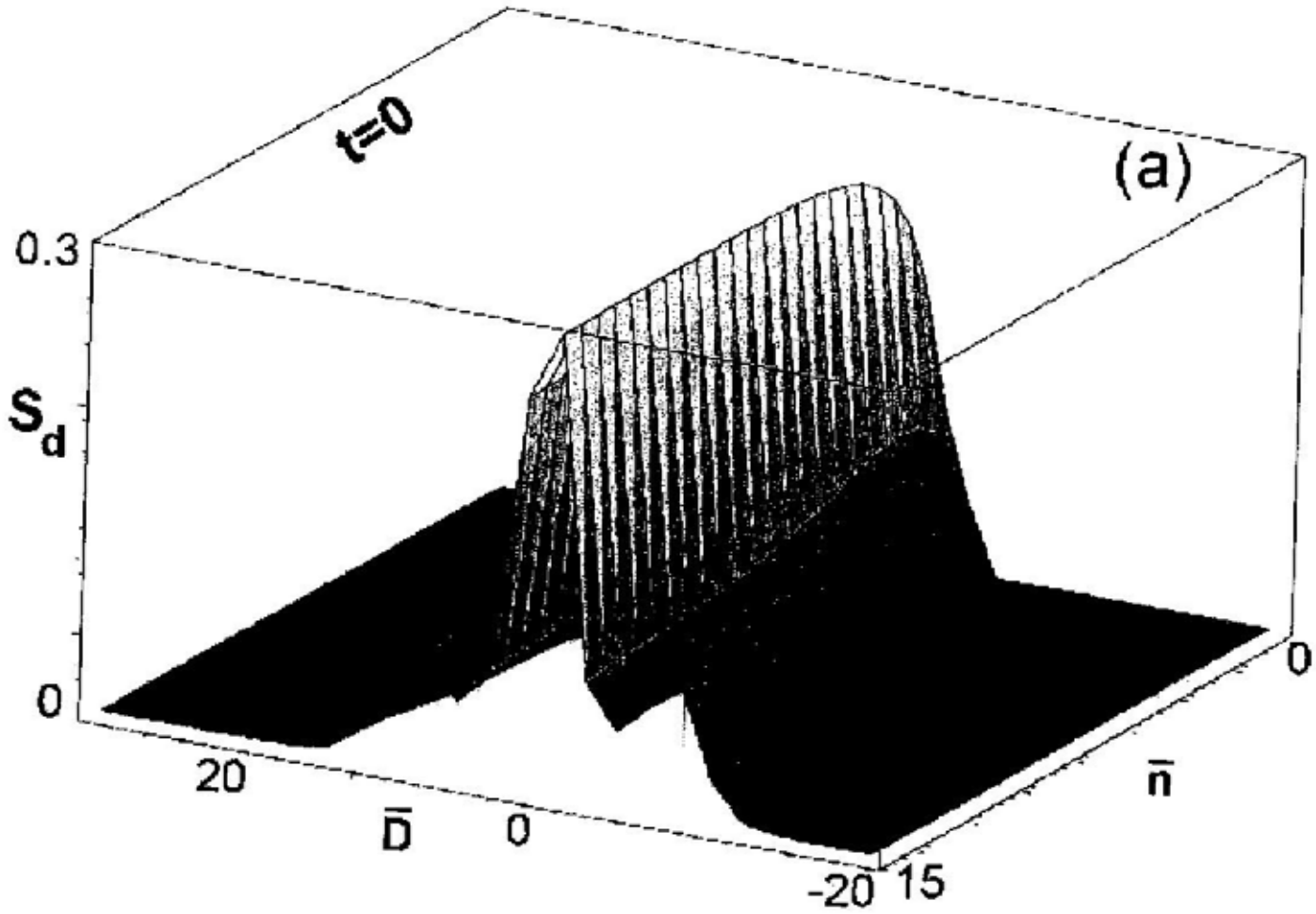


Fig.(2a)

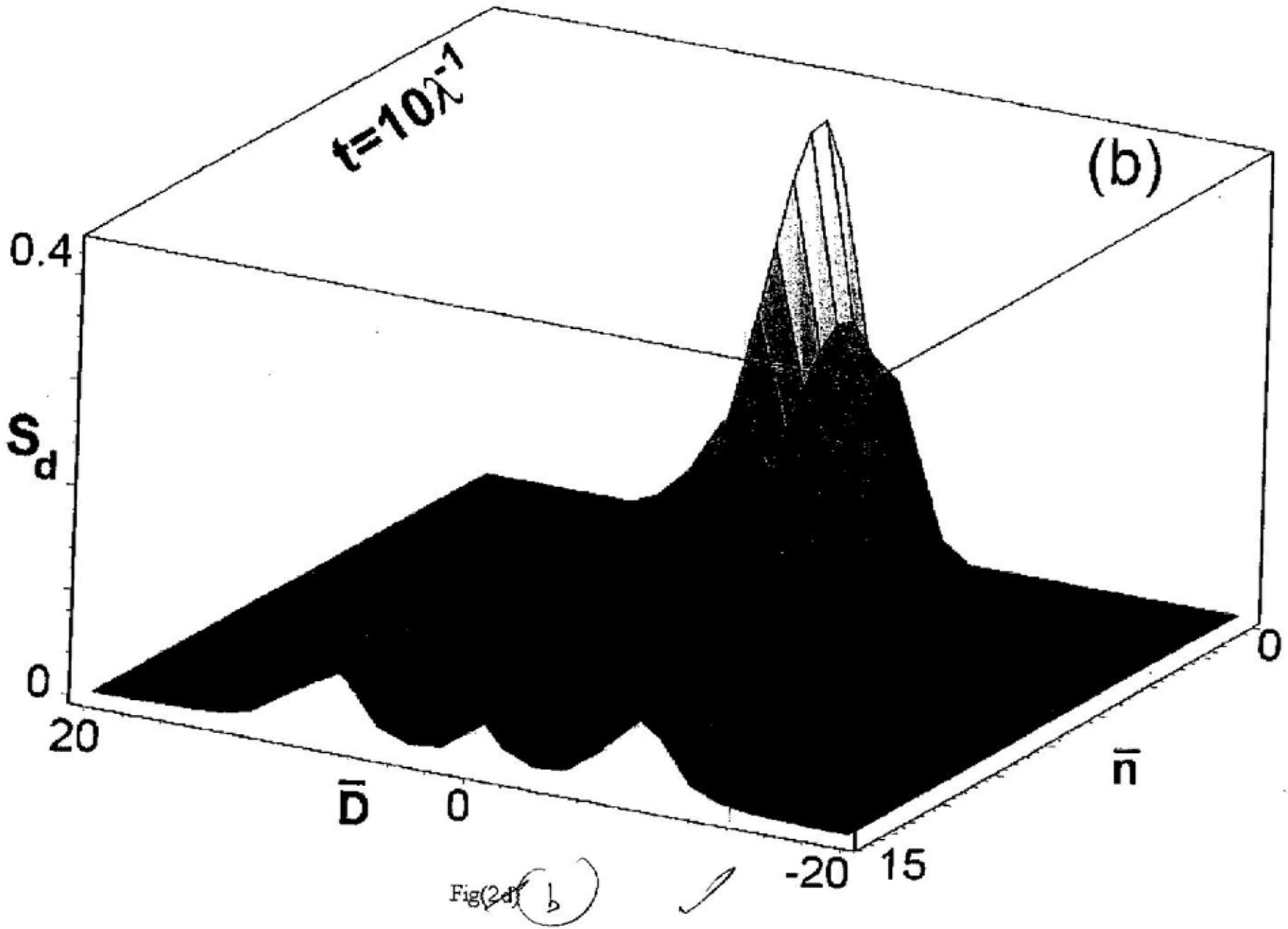


Fig(2d) b

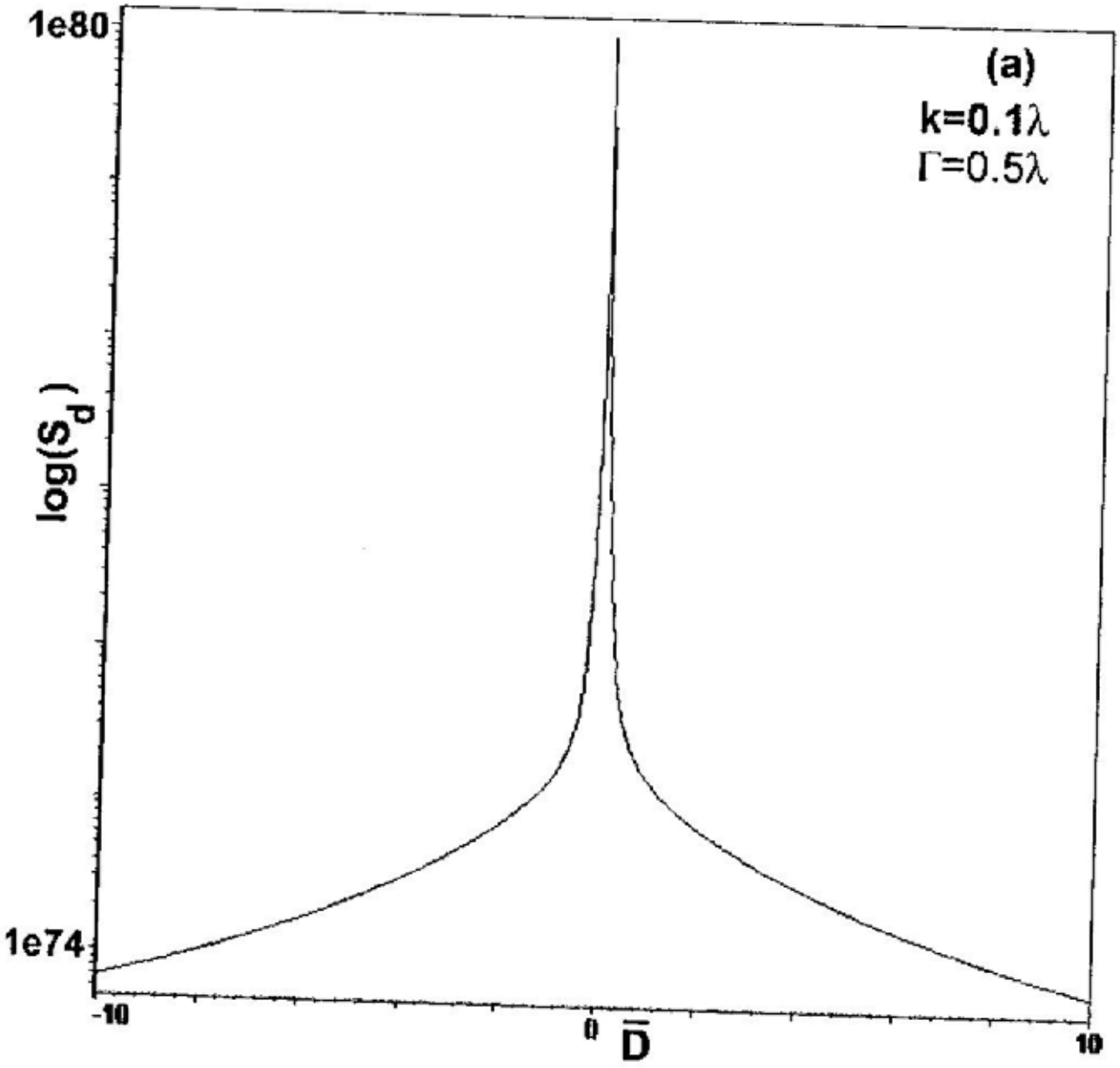


Fig(3a)

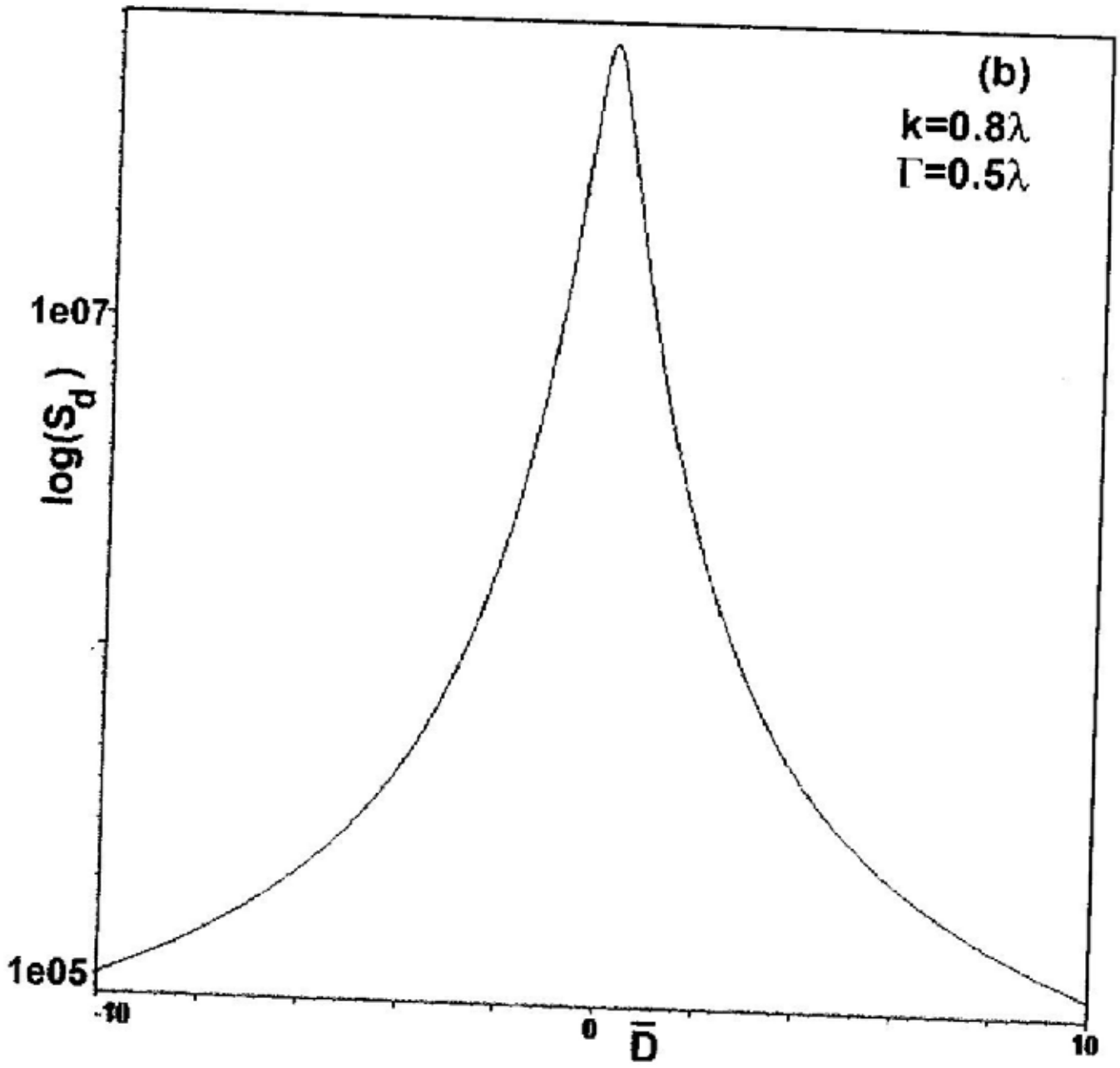


Fig(3b)

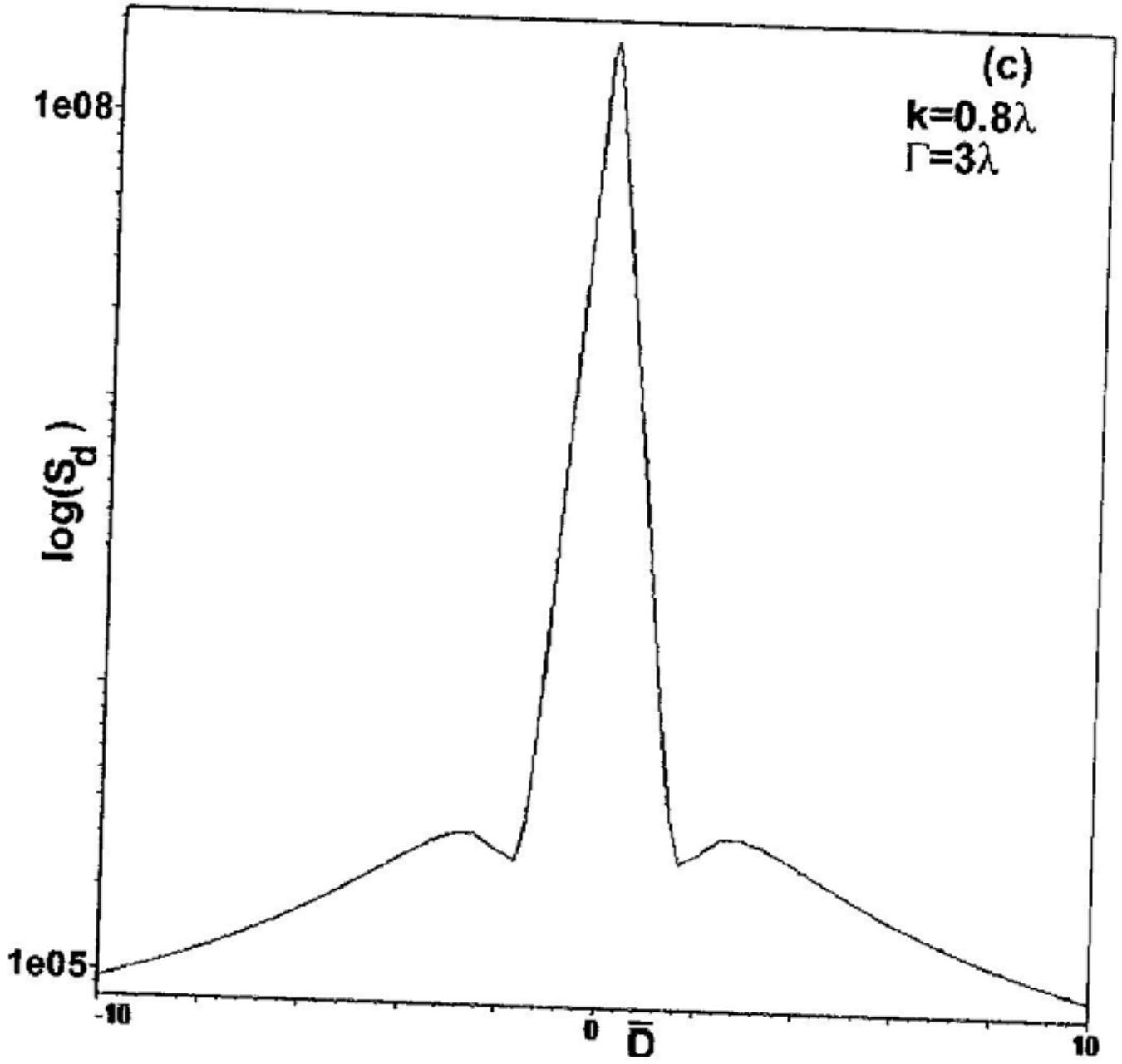


Fig(3c)

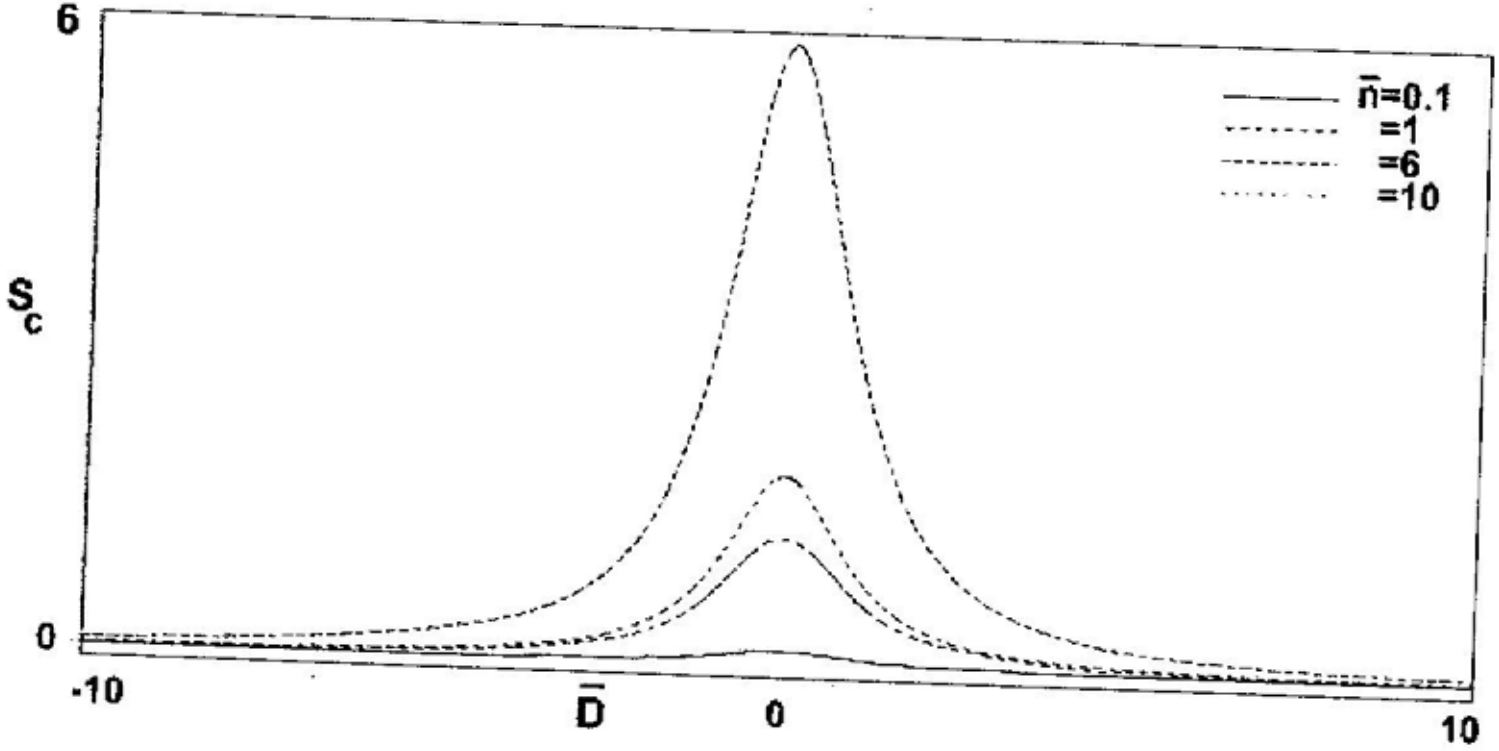


Fig(4)

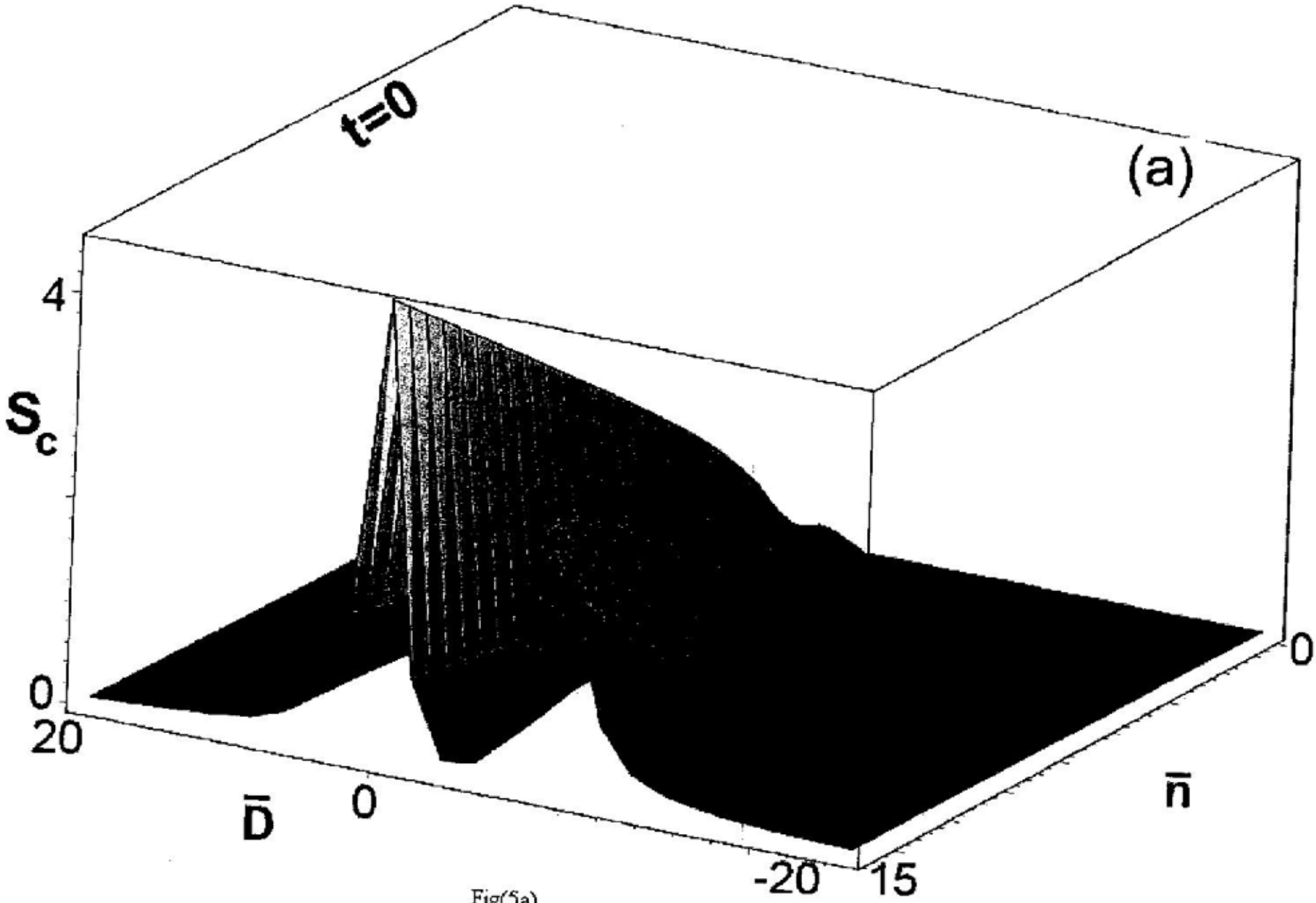


Fig(5a)

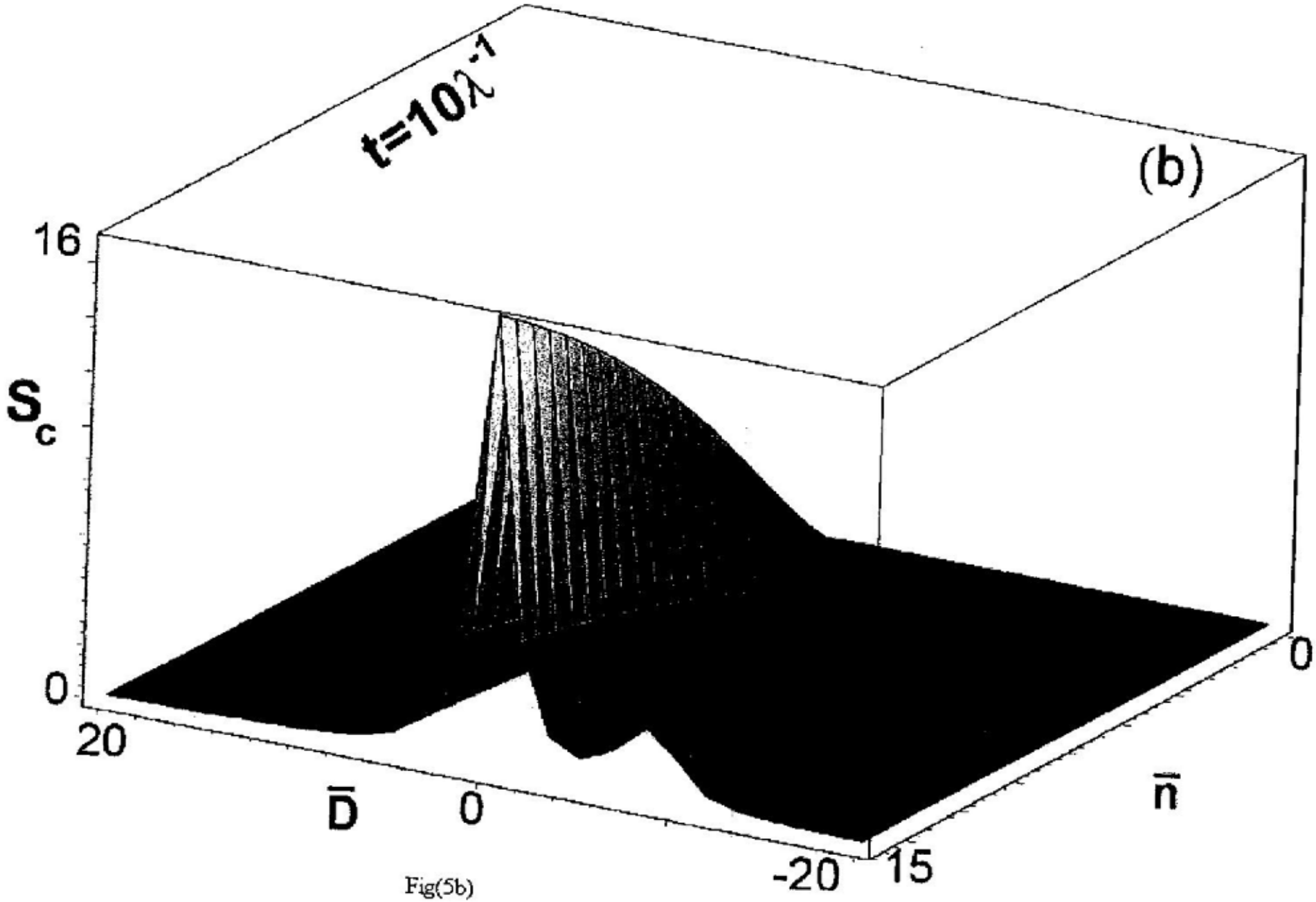


Fig(5b)

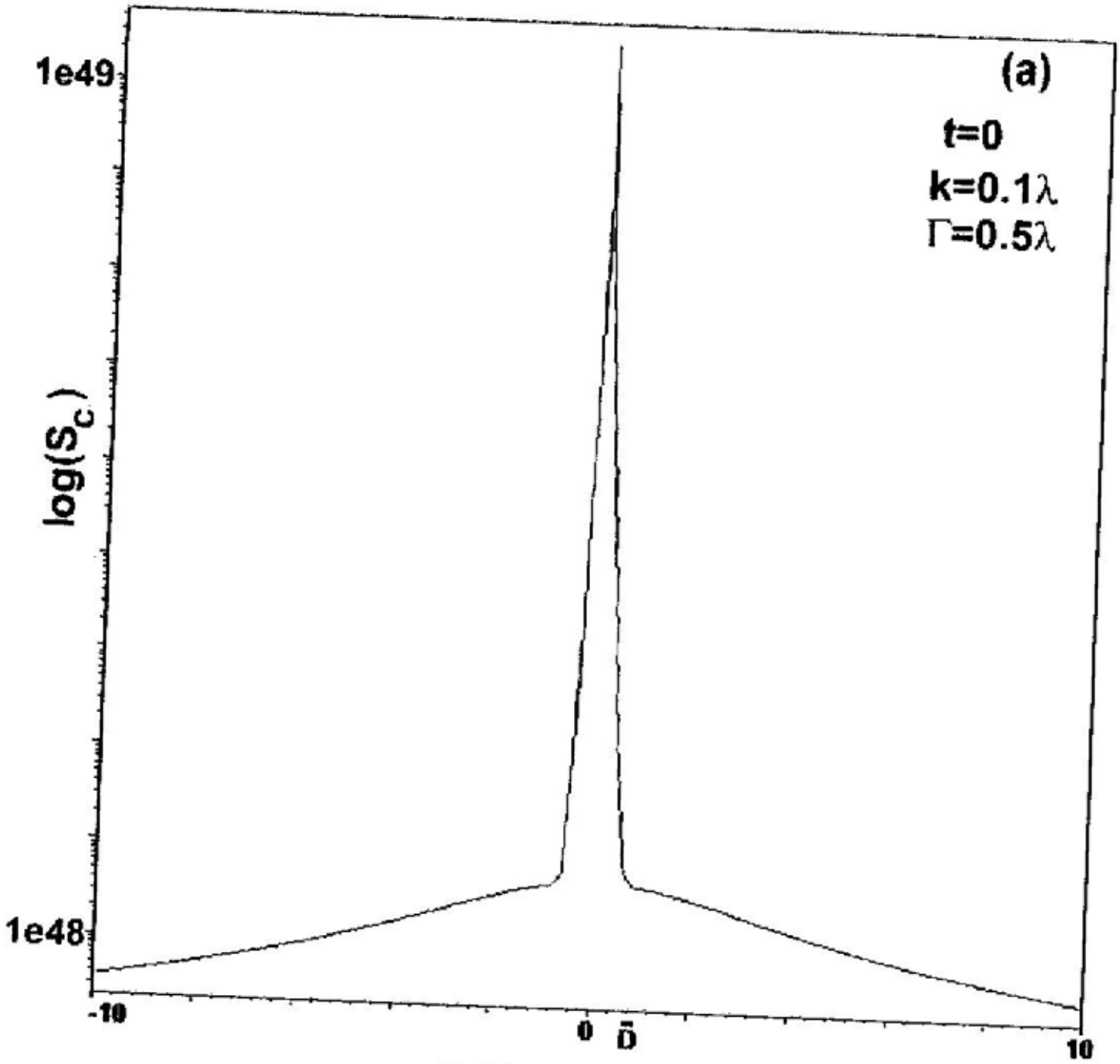


Fig(6a)

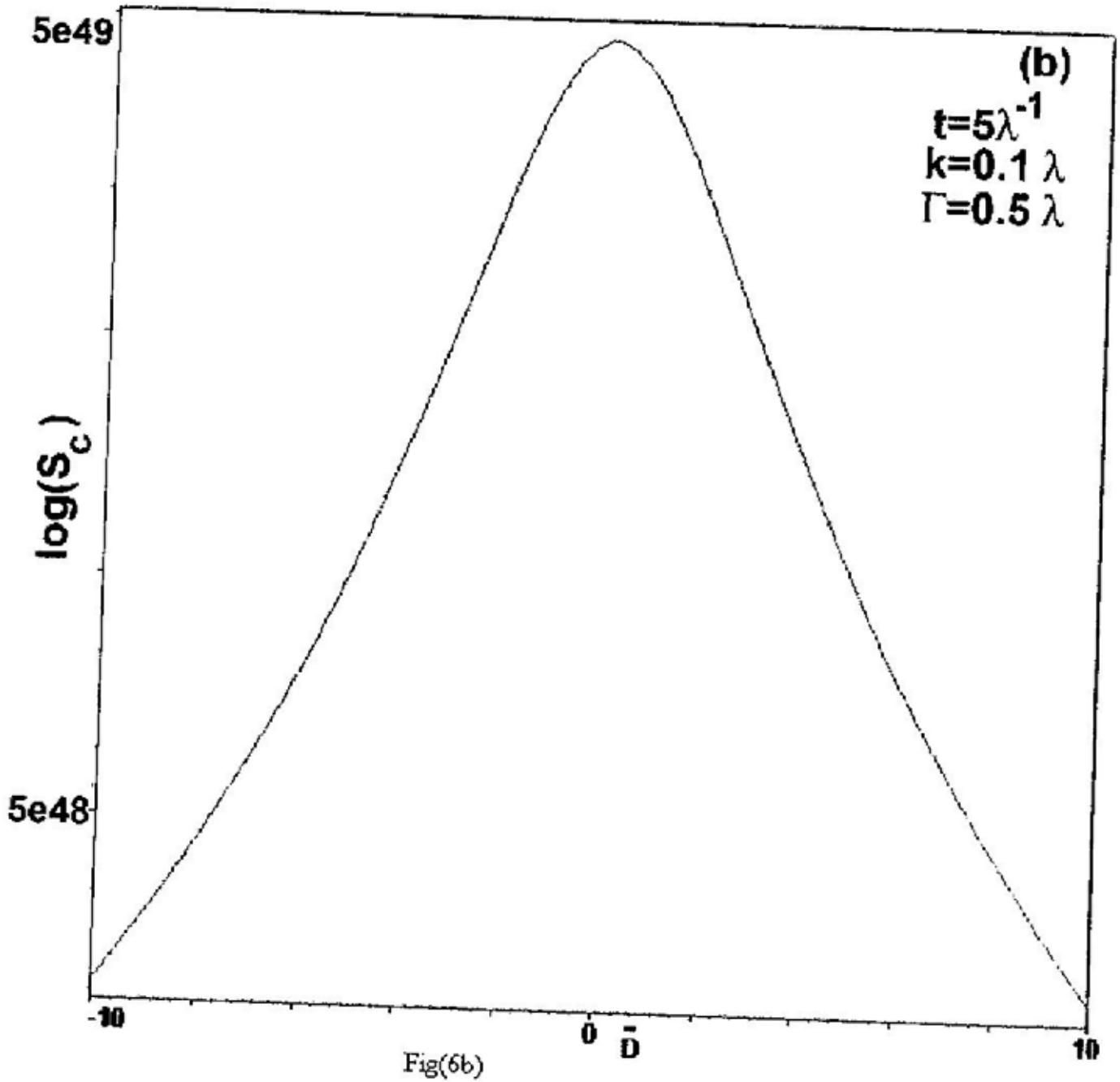


Fig(6b)

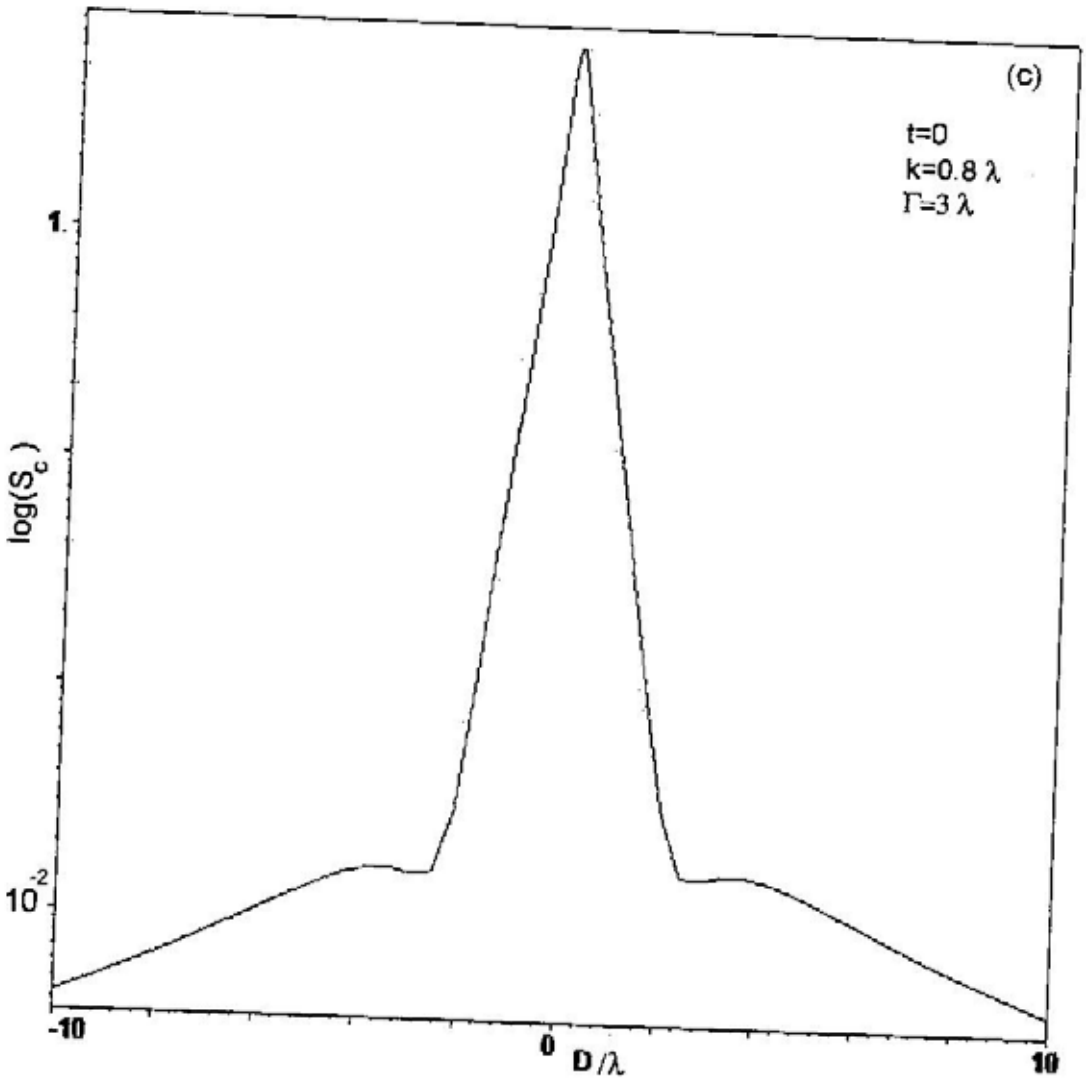
(c)
t=0
k=0.8 λ
Γ=3 λ
1
log(S_c)
10^-2
-10
0
D/λ
10

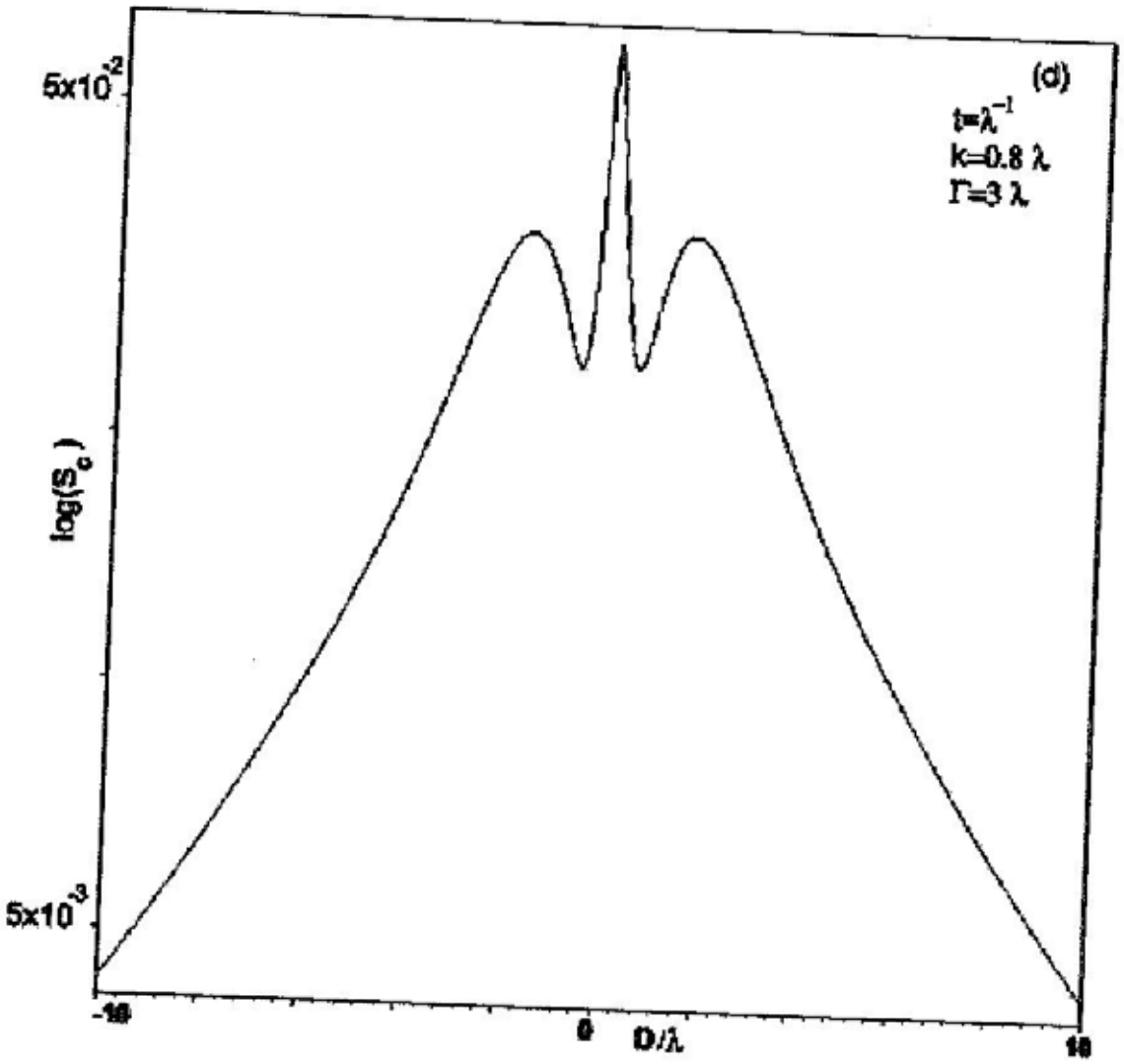
(d)
t=λ^-1
k=0.8 λ
Γ=3 λ
5x10^-2
5x10^-3
log(S_c)
-10
0
D/λ
10